

## Pattern analysis in networks of diffusively coupled Lur'e systems

Rogov, Kirill; Pogromsky, Alexander; Steur, Erik; Michiels, Wim; Nijmeijer, Henk

**DOI**

[10.1142/S0218127419502006](https://doi.org/10.1142/S0218127419502006)

**Publication date**

2019

**Document Version**

Accepted author manuscript

**Published in**

International Journal of Bifurcation and Chaos

**Citation (APA)**

Rogov, K., Pogromsky, A., Steur, E., Michiels, W., & Nijmeijer, H. (2019). Pattern analysis in networks of diffusively coupled Lur'e systems. *International Journal of Bifurcation and Chaos*, 29(14), [1950200]. <https://doi.org/10.1142/S0218127419502006>

**Important note**

To cite this publication, please use the final published version (if applicable). Please check the document version above.

**Copyright**

Other than for strictly personal use, it is not permitted to download, forward or distribute the text or part of it, without the consent of the author(s) and/or copyright holder(s), unless the work is under an open content license such as Creative Commons.

**Takedown policy**

Please contact us and provide details if you believe this document breaches copyrights. We will remove access to the work immediately and investigate your claim.

# PATTERN ANALYSIS IN NETWORKS OF DIFFUSIVELY COUPLED LUR'E SYSTEMS

Kirill Rogov, Alexander Pogromsky  
*Department of Mechanical Engineering,  
Eindhoven University of Technology, The Netherlands,  
k.rogov@tue.nl, a.pogromski@tue.nl*

Erik Steur  
*Delft Center for Systems and Control,  
Delft University of Technology, The Netherlands,  
e.steur@tudelft.nl*

Wim Michiels  
*Department of Computer Science,  
Catholic University of Leuven, Belgium,  
wim.michiels@cs.kuleuven.be*

Henk Nijmeijer  
*Department of Mechanical Engineering,  
Eindhoven University of Technology, The Netherlands,  
h.nijmeijer@tue.nl*

Received (to be inserted by publisher)

In this paper, a method for pattern analysis in networks of diffusively coupled nonlinear systems of Lur'e form is presented. We consider a class of nonlinear systems which are globally asymptotically stable in isolation. Interconnecting such systems into a network via diffusive coupling can result in persistent oscillatory behavior, which may lead to pattern formation in the coupled systems. Some of these patterns may co-exist and can even all be locally stable, i.e. the network dynamics can be multi-stable. Multi-stability makes the application of common analysis methods, such as the direct Lyapunov method, highly involved. We develop a numerically efficient method in order to analyze the oscillatory behavior occurring in such networks. We focus on networks of Lur'e systems in which the oscillations appear via a Hopf bifurcation with the (diffusively) coupling strength as a bifurcation parameter and therefore display sinusoidal-like behavior in the neighbourhood of the bifurcation point. Using the describing function method, we replace nonlinearities with their linear approximations. Then we analyze the system of linear equations by means of the multivariable harmonic balance method. We show that the multivariable harmonic balance method is able to accurately predict patterns that appear in such a network, even if multiple patterns co-exist.

*Keywords:* Periodic Solutions, Bifurcations, Harmonic Balance, Nonlinear Systems

## 1. Introduction

In recent years, the study of complex networks consisting of coupled nonlinear dynamical systems has been a significant subject in mathematical biology, control theory, applied physics, and interdisciplinary fields. Its relevance is due to several factors: complex networks are prevalent in the world (e.g. neuroscience, heart cells synchronization, social networks, flocks of birds and other kinds of collective behavior); such networks show a rich dynamic behavior and may induce a large number of different applications (see [Pikovsky *et al.*, 2001], [Strogatz, 2003] and references therein). In particular, different synchronous regimes and a *pattern formation* in coupled systems are subjects of intensive study.

Numerous activities in nature exhibit oscillatory behavior and can be described by a collection of coupled nonlinear oscillators. Due to complex dynamics and different types of coupling, various phenomena appear in nonlinear networks. An omnipresent form of interaction is a *diffusive coupling* ([Hale, 1997]), in which the feedback to each (sub)system in the network is a (weighted) sum of differences in each (sub)system's output and those of its neighbours. Networks with diffusive coupling exhibit surprisingly rich phenomena, such as synchronization ([Pogromsky & Nijmeijer, 2001]), partial synchronization ([Pogromsky *et al.*, 2011]), and formation of oscillatory patterns including standing, travelling and rotating waves (see [Golubitsky *et al.*, 1999] and [Iwasaki, 2008]). Moreover, some of these patterns may co-exist and can be stable for the same set of parameters [Nakao & Mikhailov, 2010] [Gorban *et al.*, 2015b] [Gorban *et al.*, 2015a]. These patterns arise from a *diffusion-driven instability* first discussed by [Turing, 1952]. In that research, the author "suggests that a system of chemical substances reacting together and diffusing through a tissue is adequate to account for the main phenomena of morphogenesis". Several concepts related to the chemical basis of morphogenesis (development of patterns), spatial chemical patterns, and what is now called diffusion-driven instability are introduced. In general, the pattern formation phenomenon refers to the generation of complex organization in space and time.

A nonlinear analysis of Turing instability or the diffusion-driven instability phenomenon is described in [Smale, 1976]. In this paper, an example of two diffusively coupled systems is studied. Each individual system represents a cell which is inert or dead in the sense that it is globally asymptotically stable. However, when the cells are coupled via diffusion, "the cellular system pulses (or expressed perhaps overdramatically, becomes alive!) in the sense that the concentration of enzymes in each cell will oscillate infinitely". The author poses the question of determining conditions under which the diffusive coupling leads to oscillatory behavior in the network of initially globally asymptotically stable systems. Answers to this question are found in [Yakubovich & Tomberg, 1989], [Tomberg & Yakubovich, 2000], and [Pogromsky *et al.*, 1999], and references therein.

Another related result is presented in [Pogromsky *et al.*, 2011]. In that work, the authors present conditions under which a network of systems which are globally asymptotically stable by themselves, being diffusively coupled display different synchronous regimes, such as partial synchronous oscillations. In [Lowenstein *et al.*, 1964] the same phenomenon for a neuron network is described. These conditions are related to the coupling strength between the agents of the network and network topology. When the largest eigenvalue of the coupling matrix exceeds some threshold, the (network) equilibrium loses stability via a *Hopf bifurcation* and oscillatory patterns emerge. The Hopf bifurcation changes the dynamics of the network from a stable equilibrium to oscillatory patterns.

In this work, we extend the previously obtained results. In particular, we consider the problem of *prediction* of oscillatory patterns which appear in (diffusively) coupled Lur'e systems via a Hopf bifurcation. A challenge is that there may be co-existence of different oscillatory patterns, such as an in-phase and an anti-phase synchronization, and clockwise and counterclockwise waves in a ring-like structure. Some of these co-existent patterns may be stable for the same set of parameters (coupling strength), i.e. there is multi-stability. Considering multi-stability, the application of common methods for the analysis of network behavior, such as the direct Lyapunov method and the analysis of Poincaré maps, becomes highly non-trivial.

To solve these problems, we propose an extension of the *multivariable harmonic balance* (MHB) method, which is described in [Iwasaki, 2008] for neuronal circuits called the central pattern generators (CPGs). The method allows to analyse the behavior of the complex network near the bifurcation point and to determine an oscillatory profile that approximates the output of the studied network without simulating ordinary differential equations (ODEs). Despite these advantages, the MHB method cannot be directly applied to a network consisting of diffusively coupled Lur'e systems due to different structure of (sub)systems of the network and in order to achieve the best accuracy of the approximation the coupled systems must be in the neighbourhood of the Hopf bifurcation point. Being inspired by

previous results obtained in [Pogromsky *et al.*, 2011] and [Iwasaki, 2008], we developed a new approach in order to analyze oscillatory behavior and predict the patterns with equal amplitudes for the oscillations in the complex network by means of the multivariable harmonic balance (MHB) method (see [Rogov *et al.*, 2018]). In this work, we extend our results and present an approach based on the MHB method aiming at pattern analysis with arbitrary amplitudes of oscillation in networks of (diffusively) coupled identical nonlinear systems.

This paper is organized as follows. Preliminary results and the problem statement are given in Section 2. More precisely, in Subsection 2.1, networks of Lur'e systems are introduced. Oscillatory conditions are presented in Subsection 2.2. The Harmonic Balance and the describing function methods are introduced in Subsection 2.3. The problem is formulated in Subsection 2.4. Pattern analysis using the multivariable harmonic balance is described in Section 3. There are four subsections in Section 3. Subsection 3.1 describes the multivariable harmonic balance method presented in [Iwasaki, 2008]. The MHB equation is derived in Subsection 3.2. Subsections 3.3 and 3.4 introduce the equal amplitude case and the general amplitude case, respectively. Numerical results are given in Section 4 and include results for the equal amplitude case and the general amplitude case. In Section 5, the conclusions are provided.

Throughout the paper, the following notations are used.  $I_k$  denotes the identity matrices of the size  $k \times k$ .  $\top$  stands for the transposition.  $i$  stands for the imaginary unit.  $C^1$  stands for a set of continuously differentiable functions.

## 2. Preliminaries and problem statement

In Subsection 2.1 we introduce dynamical systems and the type of coupling that form networks whose dynamics are analyzed in this work. In Subsection 2.2, conditions that guarantee the occurrence of oscillatory patterns are provided. Tools being used for the analysis of network behavior are introduced in Subsection 2.3. The formulation of the problem is given in Subsection 2.4.

### 2.1. Networks of Lur'e systems

In this paper, a method to analyze the behavior of networks consisting of identical nonlinear dynamical systems is presented. To do so, we consider a network which describes a collection of identical (diffusively) coupled (sub)systems. It is assumed that the network cannot be decomposed into two or more uncoupled networks. To turn the statements above into a mathematical description, we consider a network of  $k$  identical systems described by:

$$\begin{aligned} \dot{x}_j &= Ax_j + Bu_j, \\ u_j &= u_{cj} - \Psi(z_j), \\ z_j &= Zx_j, \\ y_j &= Cx_j, \end{aligned} \tag{1}$$

where  $j = 1, \dots, k$  stands for the node number,  $x_j(t) \in \mathbb{R}^n$  is the state of a  $j$ -th (sub)system,  $u_j(t) \in \mathbb{R}^1$  is the combined input of a  $j$ -th (sub)system which consists of two components:  $\Psi(\cdot)$  which is a continuously differentiable scalar nonlinear sector-bounded function and  $u_{cj} \in \mathbb{R}^1$  which is the input receiving data from the coupling of multiple (sub)systems,  $y_j(t) \in \mathbb{R}^1$  is the output of the  $j$ -th system used for the coupling,  $z_j \in \mathbb{R}^1$  is the argument of the nonlinearity of the  $j$ -th (sub)system and  $A, B, C, Z$  are constant matrices of appropriate dimension. Taking  $u_{cj} = 0$ , we have  $k$  isolated single input single output systems given in Lur'e form.

The (sub)systems are interconnected through linear diffusive output coupling

$$u_{cj} = \gamma(-\gamma_{j1}(y_j - y_1) - \gamma_{j2}(y_j - y_2) - \dots - \gamma_{jk}(y_j - y_k)), \tag{2}$$

where  $\gamma$  is the positive overall gain which will play the role of bifurcation parameter later on,  $\gamma_{jl}$  are non-negative constants and  $\gamma_{jl} = \gamma_{lj}$ ,  $\forall j, l$ . Moreover,  $\gamma_{jl} > 0$  if and only if the  $j$ -th and  $l$ -th nodes are connected. Graphically, the connection between the nodes  $j$  and  $l$  is represented by an edge (arrow) between  $j$  and  $l$ ; see Figure 1. We assume that the network is connected, i.e. for any two nodes there exists a path (sequence of edges) connects them.

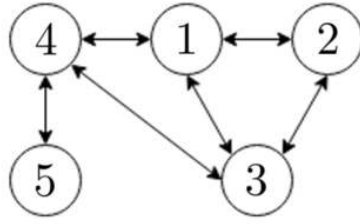


Fig. 1. An example of the network consisting of dynamical systems.

We define the coupling matrix  $\Gamma$  of size  $k \times k$  as

$$\Gamma = \gamma \begin{pmatrix} \sum_{l=2}^k \gamma_{1l} & -\gamma_{12} & \cdots & -\gamma_{1k} \\ -\gamma_{21} & \sum_{l=1, l \neq 2}^k \gamma_{2l} & \cdots & -\gamma_{2k} \\ \vdots & \vdots & \ddots & \vdots \\ -\gamma_{k1} & -\gamma_{k2} & \cdots & \sum_{l=1}^{k-1} \gamma_{kl} \end{pmatrix}. \quad (3)$$

Note that  $\Gamma = \Gamma^\top$  with all row sums zero and thus all eigenvalues are non-negative [Gershgorin, 1931]. Moreover, since we assumed that the network is connected, the matrix  $\Gamma$  has simple zero eigenvalue.

Using the Laplace transformation, the time-invariant linear part of the network (1) is rewritten into the transfer function representation, leading to the following description of the closed loop system (note that  $s$  stands for the differential operator)

$$\begin{aligned} y_j &= W_y(s)u_j, \\ z_j &= W_z(s)u_j, \\ u_j &= -\sum_{l=1}^k \gamma_{jl}y_l - v_j, \\ v_j &= \psi(z_j), \end{aligned} \quad (4)$$

with  $W_y(s)$  and  $W_z(s)$  defined as

$$W_y(s) = C(sI - A)^{-1}B, \quad (5)$$

$$W_z(s) = Z(sI - A)^{-1}B. \quad (6)$$

## 2.2. Conditions for oscillatory behavior

The goal of this subsection is to present conditions that guarantee that the network (1)-(2) exhibits oscillatory behavior. The system (1)-(2) is called *Y-oscillatory* if the system's solutions are ultimately bounded and there exist a  $j \in \{1, \dots, k\}$  such that for *almost all* initial conditions  $x(0) \in \mathbb{R}^{kn}$   $\lim_{t \rightarrow +\infty} y_j(t)$  does not exist [Yakubovich, 1973].

Networks of the form (1)-(2) were considered in [Pogromsky *et al.*, 2011] and it was shown that individual dynamics of the (sub)systems of the network satisfies some conditions for network synchronization.

**Assumption 1.** The individual dynamics of system (1) and transfer functions (5) and (6) satisfy the following conditions:

- i) Matrix  $A$  is Hurwitz, so there is a positive definite matrix  $P = P^\top$ , so that  $A^\top P + PA = -I$ ;
- ii) Matrix  $Z$  satisfies  $Z^\top = PB$  with matrix  $P$  as in i);
- iii)  $\psi(\cdot)$  is an odd, strictly increasing  $C^1$ -function with the following property  $\forall L > 0 \exists \sigma > 0$  such that  $\forall z > \sigma$   $\psi(z) > Lz$ ;
- iv) Transfer function  $W_y(s)$  is non-degenerate, has an even number of zeros with positive real part and relative degree one, and  $W_y(0) > 0$ ;
- v) Transfer function  $W_z(s)$  is such that  $W_z(0) > 0$ .

The following theorem from [Pogromsky *et al.*, 2011] provides a condition under which a network that satisfies Assumption 1, exhibits oscillatory behavior.

**Theorem 1.** *Consider a network of diffusively coupled systems of the form (4) that satisfy Assumption 1 with a symmetric coupling matrix  $\Gamma$  as in (3).*

*There is a number  $\bar{\lambda} > 0$  such that if the largest non-zero eigenvalue  $\lambda_{max}$  of  $\Gamma$  exceeds  $\bar{\lambda}$  then the network is Y-oscillatory.*

The proof of the theorem captures three points:

- i) The origin is the unique equilibrium point of the closed loop system;
- ii) The system is uniformly ultimately bounded (see [Khalil, 1996]);
- iii) The origin is hyperbolically unstable if  $\lambda_{max} > \bar{\lambda}$ , where  $\lambda_{max}$  is the largest eigenvalue of  $\Gamma$ .

Depending on the value of the parameter  $\gamma$ , the dynamics of a network has at least two different modes (a globally asymptotically stable mode and a Y-oscillatory mode). In this work, we consider the case when the oscillatory behavior is caused by a Hopf bifurcation in the network at the point  $\lambda_{max} = \bar{\lambda}$ . Therefore,  $\gamma$  is chosen to be the bifurcation parameter. The Hopf bifurcation point can be easily computed for any network consisting of nonlinear dynamical systems of the form (4). The Hopf bifurcation of an equilibrium is characterized by one bifurcation condition which is the presence of a purely imaginary pair of eigenvalues of the Jacobian matrix evaluated at this equilibrium [Kuznetsov, 1998]. For some networks the largest eigenvalue  $\lambda_{max}$  of the coupling matrix  $\Gamma$  has algebraic and geometric multiplicity larger than one (see Section 3) which corresponds to the occurrence of an *equivariant Hopf* bifurcation [Balanov, 1997]. Assuming that  $\psi'(0) = 0$ , the Hopf bifurcation (equivariant Hopf bifurcation) occurs when the matrix  $A - BC\bar{\lambda}$  has a pair of purely imaginary eigenvalues with algebraic and geometric multiplicity one (larger than one) and the other eigenvalues have negative real part. We also compute the bifurcation frequency  $\omega_{bif}$  which will be required later on.

According to normal form theory (see [Han & Yu, 2012] and references therein), the oscillations are sinusoidal-like near the bifurcation point. It justifies using the describing function method to replace the nonlinearity by its linear approximation and then to analyze the system of linear equations by means of the harmonic balance method.

### 2.3. Harmonic Balance Method

The harmonic balance method provides an analytical approximation of periodic solution(s) of an ODE and is applicable to nonlinear systems. In order to apply this method we approximate the nonlinearity  $\psi(\cdot)$  of (sub)system (1) with its describing function. Suppose a (sub)system of the Y-oscillatory network has a periodic solution  $z_j(t)$ . Then, by Fourier series expansion, we obtain

$$z_j(t) = \sum_{m=0}^{\infty} a_{jm} \sin(\omega m t) + b_{jm} \cos(\omega m t)$$

for real vectors  $a_{jm}$  and  $b_{jm}$  and frequency  $\omega$ . In the neighbourhood of the bifurcation point the solution can be approximated by its first harmonics

$$z_j(t) \cong \alpha_j \sin(\omega t + \phi_0 + \phi_j), \quad (7)$$

where  $\alpha_j$  is the amplitude,  $\omega$  is the frequency,  $\phi_0$  is the initial phase and  $\phi_j$  is the phase for the  $j$ -th (sub)system of the network. For an autonomous system we can take  $\phi_0 = 0$  without loss of generality. In order to approximate the nonlinearity  $\psi(\cdot)$ , which is assumed to be odd function, by its describing function  $k$ , we first compute the describing function which stands for the gain and then replace the nonlinearity with the linear gain as follows:

$$\psi(z_j) \cong k(\alpha_j) z_j, \quad (8)$$

where

$$k(\alpha_j) := \frac{2}{\pi \alpha_j} \int_0^{\pi} \psi(\alpha_j \sin \theta) \sin \theta d\theta, \quad (9)$$

is the describing function of  $\psi(\cdot)$ .

The describing function  $k(\alpha_j)$  stands for the average gain of the nonlinearity  $\psi(\cdot)$  when the input of the nonlinearity

is a sinusoidal signal of amplitude  $\alpha_j$  ([Khalil, 1996]). The harmonic balance method for networks of CPGs (Central Pattern Generators) [see Section 3.1 for details], called the Multivariable Harmonic Balance (MHB), was described in [Iwasaki, 2008].

## 2.4. Problem formulation

Networks of the form (1)-(2), whose (sub)system's individual dynamics satisfy Assumption 1, exhibit oscillatory behavior if the coupling between network agents is strong enough. For coupling strength slightly larger than the bifurcation point, these oscillatory patterns are characterized by a set of parameters (oscillatory profiles); amplitudes  $\alpha_j$ , phases  $\phi_j$  and frequency  $\omega$ . Some of these patterns can co-exist and can be locally stable, which implies the multi-stability of the network dynamics. Since we consider the case when oscillations appear via a Hopf bifurcation (equivariant Hopf bifurcation), the use of an approach based on the harmonic balance method is justified at least for  $\gamma$  close to the bifurcation point. The harmonic balance method helps to avoid a classical analysis, e.g., by means of the direct Lyapunov method, which is cumbersome when we deal with multi-stability. Moreover, the harmonic balance method is numerically efficient. In this paper, we consider the problem of computing approximations (7) of all patterns of oscillations in a given network.

## 3. Pattern Prediction by means of Multivariable Harmonic Balance

In this section, we review the multivariable harmonic balance (MHB) method which we extend in order to analyze the behavior of networks of the form (4) when pattern formation occurs. The MHB method approximates the behavior of a network consisting of nonlinear systems and determines an oscillatory profile (frequency  $\omega$ , amplitudes  $\alpha_j$ , phases  $\phi_j$ ) as a solution to an eigenvalue problem. In Subsection 3.1, the Multivariable Harmonic Balance described in [Iwasaki, 2008] is introduced. In Subsection 3.2, we show how the MHB method is applied to the network (1)-(2). There are two cases to discuss namely the equal amplitude case and the general amplitude case which are described in Subsections 3.3 and 3.4, respectively.

### 3.1. Multivariable Harmonic Balance

The Multivariable Harmonic Balance (MHB) developed in [Iwasaki, 2008] considers networks of identical interconnected (sub)systems described by a dynamical mapping from input  $u_j$  to output  $z_j$ :

$$z_j(s) = f(s)u_j(s), \quad u_j(s) = \sum_{l=1}^k \mu_{jl}(s)v_l, \quad v_j = \Psi(z_j),$$

where  $f(s)$  is a rational transfer function of variable  $s$ , which represents the linear time-invariant part of each (sub)system,  $\Psi(z_j)$  is a continuously differentiable odd static nonlinear function,  $z_j(s)$  is the  $j$ -th (sub)system output and  $\mu_{jk}(s)$  is a transfer function representing the connection from  $k$ -th system to  $j$ -th system. In vector form, these dynamics can be written as

$$z = F(s)u, \quad u = M(s)v, \quad v = \Psi(z), \quad (10)$$

where  $\Psi(z) := \text{col}[\Psi(z_1), \dots, \Psi(z_k)]$ ,  $z := \text{col}[z_1, \dots, z_k]$ ,  $F(s) := f(s)I_k$  and  $M(s)$  is the transfer matrix of the coupling whose  $(j, k)$  entry is  $\mu_{jk}(s)$ . Using equations (7)-(9), the dynamic equations are approximated by the MHB equation

$$(\mathcal{M}(s)\mathcal{K}(\alpha) - I_k)q = 0, \quad q_j := \alpha_j e^{i\phi_j}, \quad q \in \mathbb{C}^k, \quad (11)$$

where  $\mathcal{M}(s) = F(s)M(s)$ ,  $\mathcal{K}(\alpha) := k(\alpha_j)I_k$  is a diagonal matrix and  $q$  is a solution to the eigenvalue problem. The MHB equation characterizes the oscillatory profiles for (10) as follows. In order to obtain approximations of oscillatory solutions, we substitute a sample solution of the form  $q_j = \alpha_j \exp(i\phi_j)$ . All three components ( $\alpha$ ,  $\phi$ ,  $\omega$ ) of the pattern are computed and the oscillatory profile is reconstructed using (7).

In general, the MHB equation is nonlinear in  $\alpha$  and might have multiple solutions and it is necessary to determine the stable oscillations. In order to examine stability of such oscillatory solution, we use an approximate method from [Glad & Ljung, 2000] commonly accepted in the engineering literature. Based on (8), we consider the linear systems

obtained by replacing the nonlinearity  $\Psi$  with constant gain  $\mathcal{K}(\alpha)$  as follows.

$$L_K := \begin{cases} z = \mathcal{M}(s)v, \\ v = \mathcal{K}(\alpha)z. \end{cases} \quad (12)$$

The block scheme representation of the linear system  $L_K$  is illustrated in Figure 2. From the perspective of the describing function method, the linear system  $L_K$  contains some information on the network behavior when its oscillations are sinusoidal-like with a set of amplitudes  $\alpha$ . According to the approximate method from [Glad & Ljung, 2000], the oscillation with certain  $\omega, \alpha, \phi$  is stable if the linear approximation  $L_K$  is marginally stable, which is equivalent (if linear system has pure imaginary eigenvalues) to the boundedness of all solutions of (12).

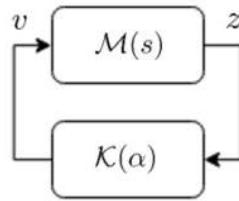


Fig. 2. Linear system  $L_K$ .

From the above, the key ideas of the MHB analysis are summarised as follows:

- The oscillatory profile can be obtained by solving equation (11) for frequency  $\omega$  and eigenvector  $z$  containing encoded amplitudes and phases.
- The predicted oscillatory pattern is stable if the corresponding linear system  $L_K$  given in (12) with  $K := \mathcal{K}(\alpha)$  is marginally stable with a pair (pairs) characteristic roots at  $s = \pm i\omega$  on the imaginary axis and with the rest characteristic roots located in the open left half plane.

### 3.2. Deriving the MHB equation

It is shown that the MHB method turns the problem of determining oscillatory profiles into an eigenvalue problem. System (4) does not belong to the class of systems considered in [Iwasaki, 2008], so the previously described MHB method cannot be directly applied. In [Iwasaki, 2008], it was considered the case of linear system dynamics with nonlinear coupling and we deal with nonlinear system dynamics with diffusive linear coupling. In order to apply the MHB analysis, a loop transformation is performed. Figure 3 displays how the loop transformation reorders the structure of the network. The left and right blocks describe the networks (4) and (10), respectively.

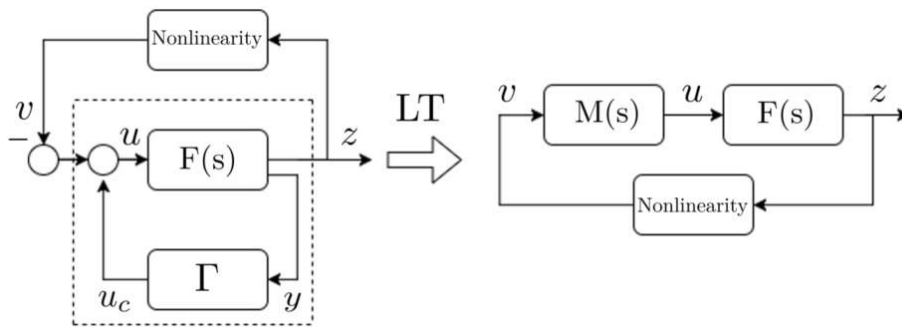


Fig. 3. Loop Transformation reorders the structure of the network in order to apply the MHB method.



The following manipulations are performed to turn system (4) into the form of (10). Recall System (4) and rewrite the input  $u$  in vector form as

$$\begin{aligned} u &= -W_y(s)\Gamma u - v, \\ W_y(s) \left[ \frac{1}{W_y(s)} I_k + \Gamma \right] u &= -v, \end{aligned}$$

with matrix  $\Gamma$  defined in (3). Defining the resolvent  $R\left(\frac{1}{W_y(s)}\right) = \left[\frac{1}{W_y(s)} I_k + \Gamma\right]^{-1}$ , we obtain

$$u = -\frac{1}{W_y(s)} R\left(\frac{1}{W_y(s)}\right) v.$$

The network now takes the form of (10) with

$$\begin{aligned} F(s) &= W_z(s)I_k, \\ M(s) &= -\frac{1}{W_y(s)} \left[ \frac{1}{W_y(s)} I_k + \Gamma \right]^{-1}. \end{aligned} \tag{13}$$

Combining the second equation from (10) with (13) and replacing  $s$  by  $i\omega$ , we arrive at the following equation

$$\mathcal{M}(i\omega) = -\frac{F(i\omega)}{W_y(i\omega)} \left( \frac{1}{W_y(i\omega)} I_k + \Gamma \right)^{-1}.$$

Define the diagonal matrix

$$H(i\omega) := \frac{F(i\omega)}{W_y(i\omega)} = \left( \frac{W_z(i\omega)}{W_y(i\omega)} \right) I_k$$

and substitute it in the previous equation in order to obtain

$$\mathcal{M}(i\omega) = -H(i\omega) \left( \frac{1}{W_y(i\omega)} I_k + \Gamma \right)^{-1}.$$

Subsequently, we rewrite the MHB equation (11) as follows

$$\mathcal{M}(i\omega)(\mathcal{K}(\alpha) - \mathcal{M}^{-1}(i\omega))q = 0,$$

where  $\mathcal{M}^{-1}(i\omega) = -\left(\frac{1}{W_y(i\omega)} I_k + \Gamma\right)H(i\omega)^{-1}$  and expand it in order to obtain

$$\mathcal{M}(i\omega) \left( \frac{W_z(i\omega)}{W_y(i\omega)} \right) \left[ \mathcal{K}(\alpha) \left( \frac{W_z(i\omega)}{W_y(i\omega)} \right) + \frac{1}{W_y(i\omega)} I_k + \Gamma \right] q = 0.$$

Since  $\mathcal{M}(i\omega)(W_z(i\omega)/W_y(i\omega))$  is non-singular for  $\omega > 0$ , we obtain

$$J(\alpha, \omega)q := \left[ \mathcal{K}(\alpha) \left( \frac{W_z(i\omega)}{W_y(i\omega)} \right) + \frac{1}{W_y(i\omega)} I_k + \Gamma \right] q = 0, \quad q_j := \alpha_j e^{i\phi_j} \tag{14}$$

which is the multivariable harmonic balance equation for the networks of identical Lur'e systems. We focus on determining patterns that appear in such networks. We consider both the equal amplitude case with  $\alpha_j = \alpha_e \forall j$ , and some  $\alpha_e \in \mathbb{R}^+$ , and the general amplitude case with possibly (all) different  $\alpha_j \in \mathbb{R}^+$ ,  $j = 1, \dots, k$ .

### 3.3. Equal amplitude case

In this subsection we review the equal amplitude case to gain some insight into the method. This special case is derived for networks exhibiting oscillations with equal amplitudes  $\alpha_j = \alpha_e \forall j$ . In particular, we consider ring-like networks with three and four nodes (Fig.4). Each (sub)system of these networks is a dynamical system that satisfies Assumption 1 and whose dynamics are presented in Section 4. The network topology is represented by a symmetric unweighted graph with the overall coupling gain, which means that  $\gamma_{jl} = 1$  if there is the connection between the  $j$ th and  $l$ th nodes and  $\gamma_{jl} = 0$  otherwise. The nodes are interconnected with neighbours via diffusive coupling. According to this, considered networks are regular in the following sense: Networks are referred to as regular if each node has exactly the same number of links [Chen, 1997]. Regularity favours the occurrence of stable oscillations with equal

amplitudes. Since we look for  $\alpha_j = \alpha_e \forall j$ , the analysis of the network behavior can be substantially simplified using the structural properties of the network. In this subsection, it is shown how the oscillatory profile is determined by the MHB method for the equal amplitude case.

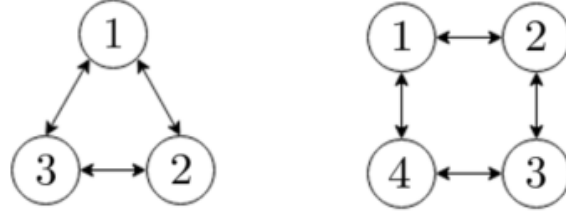


Fig. 4. Ring-like networks of diffusively coupled systems displaying oscillations with equal amplitudes

Fig. 5 reflects the oscillatory patterns that can be observed in the networks shown in Fig.4. Oscillatory profiles are obtained by direct simulation of ordinary differential equations (ODEs) of network (1). For presentation purposes, components of  $z_j(t)$  are shifted to  $z_j(t) + (k + 1 - j)$ . The oscillatory pattern has equal amplitudes with a phase shift of 120 degrees for the three-node configuration which is a rotating wave. A standing wave is observed for the four-node configuration. There are two synchronized groups of nodes which are in antiphase with each other.

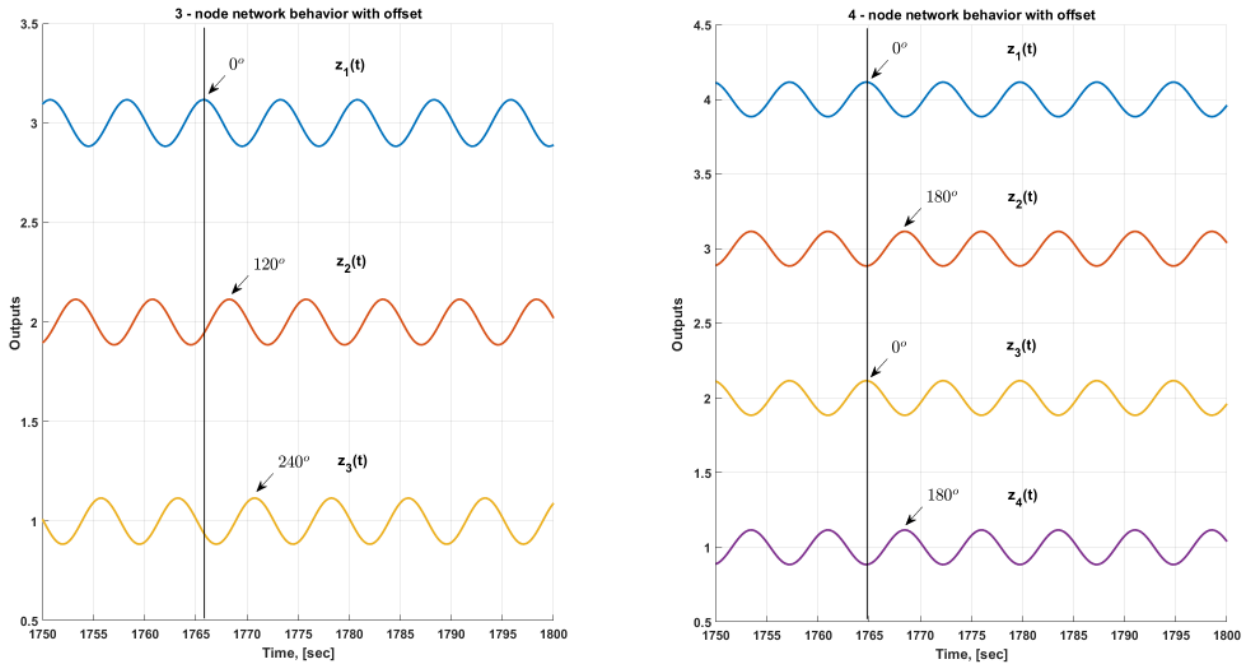


Fig. 5. Oscillatory patterns with equal amplitudes in ring-like networks (left fig.: 3-node network, right fig.: 4-node network). Network dynamics is given in Section 4.

Since we look for equal amplitudes  $\alpha_j = \alpha_e \forall j$ , the describing function matrix  $\mathcal{K}(\alpha) = k(\alpha_e)I_k$  and equation (14) reduces to

$$\left[ \frac{k(\alpha_e)W_z(i\omega) + 1}{W_y(i\omega)} I_k + \Gamma \right] q = 0, \quad q_j := \alpha_e e^{i\phi_j}, \quad (15)$$

where  $q$  is the solution to the eigenvalue problem. One can see that equation (15) has several solutions. The trivial solution  $q = 0$  corresponds to the equilibrium and is not point of interest. Therefore, we solve

$$\det \left[ \frac{k(\alpha_e)W_z(i\omega) + 1}{W_y(i\omega)} I_k + \Gamma \right] = 0.$$

After diagonalizing the coupling matrix  $\Gamma$  via a similarity transformation, which is possible due to  $\Gamma = \Gamma^\top$ , and using the property of the determinant product, we arrive at

$$\frac{k(\alpha_e)W_z(i\omega) + 1}{W_y(i\omega)} + \lambda_j = 0, \quad (16)$$

where  $\lambda_j$  is an eigenvalue of the coupling matrix  $\Gamma$ .

The described procedure implies that different oscillatory patterns may appear based on each eigenpair (an eigenvalue and its corresponding eigenvector) of the matrix  $\left[ \frac{k(\alpha_e)W_z(i\omega) + 1}{W_y(i\omega)} I_k + \Gamma \right]$ . Nonetheless, from *Theorem 1*, it is known that if  $\lambda_{max}$  exceeds some threshold the network is Y-oscillatory. It was mentioned above that an oscillation is expected to be stable if the linear approximation (12) is marginally stable. Since  $\Gamma = \Gamma^\top$ , the eigenvalues located on the imaginary axis, have linearly independent eigenvectors which are eigenvectors of the coupling matrix  $\Gamma$ . The eigenvalue with the largest real part  $\lambda_{max}$  of the coupling matrix  $\Gamma$  characterizes the Hopf bifurcation (equivariant Hopf bifurcation) point in the network. We now consider equation (16) for  $\lambda_{max}$

$$\frac{k(\alpha_e)W_z(i\omega) + 1}{W_y(i\omega)} + \lambda_{max} = 0. \quad (17)$$

Substituting (5) and (6) into (17), we obtain

$$\begin{aligned} k(\alpha_e)Z(i\omega I_n - A)^{-1}B + 1 + \lambda_{max}C(i\omega I_n - A)^{-1}B &= 0, \\ 1 + (k(\alpha_e)Z + \lambda_{max}C)(i\omega I_n - A)^{-1}B &= 0. \end{aligned}$$

Since the isolated system is exponentially stable,  $\det(i\omega I_n - A) \neq 0$  for all  $\omega$ , we have

$$(i\omega I_n - A)[1 + (k(\alpha_e)Z + \lambda_{max}C)(i\omega I_n - A)^{-1}B] = 0.$$

Using Schur's Lemma (see [Dummit & Foote, 1999]), we arrive at

$$\det[i\omega I_n - A + B(k(\alpha_e)Z + \lambda_{max}C)] = 0.$$

Thus the matrix  $A - B(k(\alpha_e)Z + \lambda_{max}C)$  has a pair of pure imaginary eigenvalues with algebraic and geometric multiplicity one for Hopf bifurcation (larger than one for equivariant Hopf bifurcation) for  $\pm i\omega$ , where  $\omega$  stands for frequency of the oscillations and the other eigenvalues are in the open left-half complex plane

$$\text{Re}(\lambda_{1,2}(A - B(k(\alpha_e)Z + \lambda_{max}C))) = 0. \quad (18)$$

In other words,  $k(\alpha_e)$  and  $\omega$  can be derived from the Hopf bifurcation condition. Now two components of the oscillatory profile are obtained:  $\alpha_e$  using (9) and  $\omega$ . The phases  $\phi_j$  are encoded in the eigenvector that corresponds to the largest eigenvalue  $\lambda_{max}$  of the coupling matrix  $\Gamma$ .

Substituting  $(k(\alpha_e)W_z(i\omega) + 1)/W_y(i\omega) = -\lambda_{max}$  in (15), we obtain

$$[\Gamma - \lambda_{max}I_k]q = 0. \quad (19)$$

Since we look for equal amplitudes, we need such eigenvector  $q$  with the entries represented as  $q_j = \alpha_j \exp(i\phi_j)$  that all elements of  $q_j$  have the same modulus  $\alpha_e$ . In order to determine the phases from the eigenvector the following equation is used

$$\phi_j = \arg(q_j). \quad (20)$$

Having all components of the oscillatory profile computed, the approximation of the oscillatory pattern of the given network using the equation (7) can be constructed.

It was mentioned above that multiple oscillatory patterns occurring in such networks may co-exist. Co-existence implies that there simultaneously exist at least two stable solutions in ring-like structured networks, such as clockwise and counter-clockwise rotating waves. This happens when the largest eigenvalue  $\lambda_{max}$  of the coupling matrix  $\Gamma$

has algebraic and geometric multiplicity two which implies the existence of two linearly independent eigenvectors corresponding to this eigenvalue or, in other words, an equivariant Hopf bifurcation occurs [Balanov, 1997]. The phases of clockwise and counter-clockwise rotating waves are encoded in these eigenvectors and be determined using (20).

### 3.4. General amplitude case

In this subsection a method for estimating the profile of oscillations with arbitrary amplitudes is presented. Networks exhibiting oscillatory patterns with different amplitudes can be easily obtained by attaching additional nodes to the networks presented in Fig.4 as shown in Fig.6. These networks consist of identical dynamical systems that satisfy Assumption 1 and whose individual dynamics is given in Section 4. As in the equal amplitude case, we consider networks whose topology is described by a symmetric unweighted graph with the overall coupling gain. Unlike the equal amplitude case, these networks are not regular.

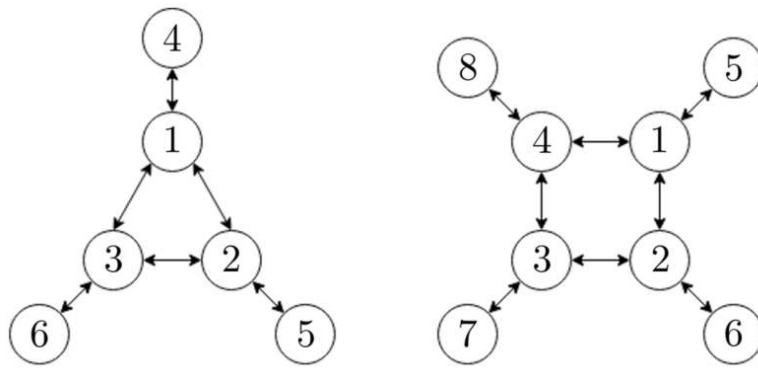


Fig. 6. Networks of identical diffusively coupled systems displaying oscillations with unequal amplitudes.

Such networks are perfect candidates to illustrate and study the general amplitude case due to their structure and behavior. Fig. 7 reflects the oscillatory patterns that can be observed in the networks shown in Fig.6. Results are obtained by the direct simulation. For presentation purposes, components of  $z_j(t)$  are shifted to  $z_j(t) + (k+1-j)$ . Two groups of nodes with equal amplitudes are observed. The first group corresponds to the core ring which is the subnetwork of nodes with more than one neighbour. Core rings of the networks from Fig.6 belong to the first group and the attached nodes belong to the second group.

Recall equation (14),

$$J(\alpha, \omega)q := \left[ \mathcal{K}(\alpha) \left( \frac{W_z(i\omega)}{W_y(i\omega)} \right) + \frac{1}{W_y(i\omega)} I_k + \Gamma \right] q = 0.$$

To solve the equation above, we formulated it as an optimization problem. Since the trivial solution  $q = 0$  is not a point of interest, we look for a set of phases  $\phi_j$ , amplitudes  $\alpha_j$  and frequency  $\omega$  which solves the nonlinear equation (14). Define the objective function to minimize as

$$F(g) := Q'Q + p^\top p, \quad (21)$$

where

$$g := [\phi; \alpha; \omega] \in \mathbb{R}^{2k+1}, \quad Q := J(\alpha, \omega)q \in \mathbb{C}^k, \quad p := \alpha - |q| \in \mathbb{R}^k,$$

where  $|q| = [|q_1|, |q_2|, \dots, |q_k|]^\top$ .

The vector  $g$  contains unknown phases, amplitudes and frequency, the component  $p$  represents the second equation of (14). To simplify the problem the phase of the first node is fixed at  $\phi_1 = 0$  and boundaries are chosen as:  $\phi_j \in [0, 2\pi] \forall j \neq 1$ ,  $\alpha_j \in [0, \beta] \forall j$ ,  $\omega \in [0, 2\omega_{bif}]$ , where  $\beta$  is a heuristically chosen number. A smart choice of  $\beta$  allows a substantial reduction in convergence time.

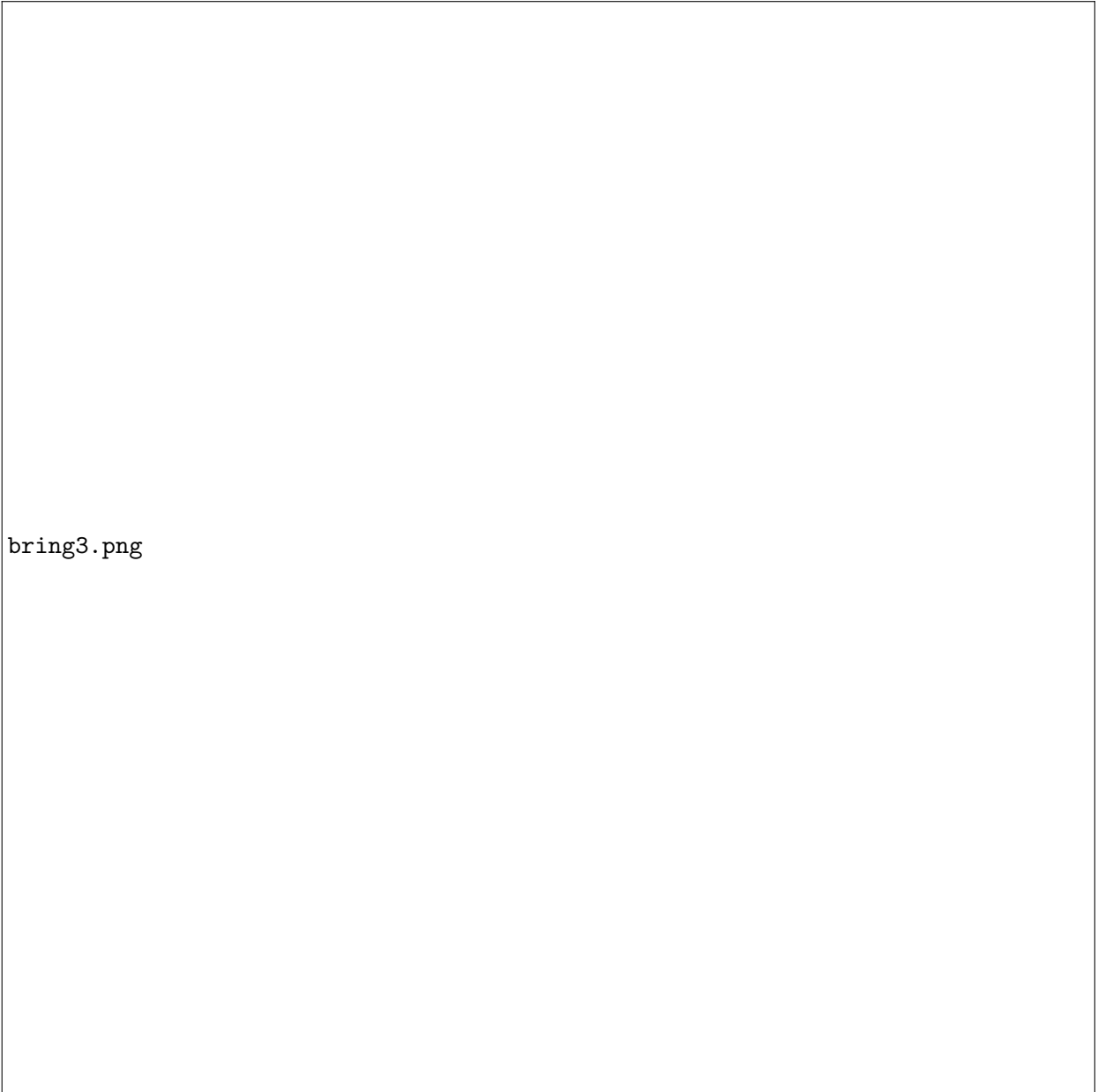


Fig. 7. Oscillatory patterns with unequal amplitudes (left fig.: 6-node network, right fig.: 8-node network). Network dynamics is given in Section 4.

Solutions to the nonlinear equation (14) are found by minimizing the squared residual norm of the objective function (21). The local solver `fmincon` included in MATLAB environment [MATLAB, 2017] is used. The solver uses the *interior-point* algorithm [Byrd *et al.*, 2000] in order to find a minimum of constrained nonlinear multivariable function in defined feasible region. Since equations (14) are nonlinear and multiple solutions exist, the solutions heavily depend on the initial conditions. Multiple values of the initial conditions are generated by the `MultiStart` algorithm [Ugray *et al.*, 2007].

A big advantage of the `MultiStart` method is that start points for the minimization procedure are not needed to be specified. A set of random points is used as initial conditions. The key point in the procedure is to choose the correct boundaries for the start points and the unknown variables.

The procedure has the following steps:

- (1) Define the objective function to minimize;

- (2) Define the constraints for start points and unknowns;
- (3) Set start points for the solver (random or custom);
- (4) Run the solver.

Moreover, the `MultiStart` algorithm can deal with multi-stability. Stable clockwise and counter-clockwise wave-like solutions can be simultaneously found.

#### 4. Numerical examples

In this section, it is shown how the multivariable harmonic balance method is applicable to networks consisting of dynamical systems of Lur'e form whose structures given in the Figures 4 and 6. These networks are perfect candidates to demonstrate the performance of the method. The networks exhibit different oscillatory patterns, such as patterns with equal and unequal amplitudes, patterns with a simple phase shift (180 degrees) and with non-trivial phase shift (e.g. 120 degrees), and co-existing clockwise and counter-clockwise wave-like patterns. The individual dynamics of the nodes, as in [Pogromsky *et al.*, 2011], is given in (1) with

$$A = \begin{pmatrix} 1 & -1 & 1 \\ 1 & 0 & 0 \\ -4 & 2 & -3 \end{pmatrix}$$

$$B = (0 \ 0 \ 1)^\top, \quad C = (0 \ 0 \ 1), \quad Z = B^\top P,$$

where  $P$  is the solution to the Lyapunov equation

$$A^\top P + PA = -I_3.$$

The nonlinear function  $\psi(\cdot)$  is given as follows

$$\psi(z_j) = z_j^3;$$

and computing the describing function by (9), we obtain

$$k(\alpha_j) = \frac{3}{4} \alpha_j^2.$$

The presented setting satisfies the conditions from *Assumption 1*. Since numerical methods are employed, it implies that a computational error exists which is given as residual of Eq.(14). In order to show, that the MHB method accurately predicts oscillatory patterns, the reconstructed oscillations and the output of a direct simulation are compared. The direct simulation results are obtained using a nonstiff differential equation solver of medium order `ode45` included in MATLAB environment [Dormand & Prince, 1980]. In order to measure the accuracy of the method we provide residual norm of the MHB equation and compare amplitudes and frequency with the ones that are extracted from ODE simulation as follows.

$$\begin{aligned} \Delta\alpha &= 100 \|\alpha - \alpha_s\| / \|\alpha_s\|; \\ \Delta\omega &= 100(\omega - \omega_s) / \omega_s, \end{aligned}$$

where  $\alpha_s$  and  $\omega_s$  are taken from the simulation. In the following two subsections, we will present results of the analytical approach for the equal amplitude case and the numerical approach for the general amplitude case.

##### 4.1. Results for the equal amplitude case

In this subsection, we show that it is possible to predict patterns occurring in regular networks with certain symmetry and that oscillatory patterns possess equal amplitudes. An example of such networks is given in the Figure 4. It is shown how to refine an oscillatory profile of the given network by means of the analytical approach presented above. This approach is applicable only for networks exhibiting patterns with equal amplitudes.

The coupling topology of the networks are given by matrices  $\Gamma_3$  and  $\Gamma_4$  where a subscript denotes the number of nodes in the network

$$\Gamma_3 = \gamma_3 \begin{pmatrix} 2 & -1 & -1 \\ -1 & 2 & -1 \\ -1 & -1 & 2 \end{pmatrix}, \quad \Gamma_4 = \gamma_4 \begin{pmatrix} 2 & -1 & 0 & -1 \\ -1 & 2 & -1 & 0 \\ 0 & -1 & 2 & -1 \\ -1 & 0 & -1 & 2 \end{pmatrix},$$

where  $\gamma_{3,4}$  are bifurcation parameters. In the Section 2, it is shown that the Hopf bifurcation (equivariant Hopf bifurcation) occurs in the network when the largest eigenvalue  $\lambda_{max}$  with algebraic and geometric multiplicity one (larger than one) of the coupling matrix parametrized by bifurcation parameter  $\gamma$  exceeds some threshold  $\bar{\lambda}$ . Parameters  $\bar{\lambda}_3, \bar{\lambda}_4$  can be calculated from the Hopf bifurcation (equivariant Hopf bifurcation) condition  $A - BC\bar{\lambda}$  described in Section 2.2 and for the given networks these are:  $\bar{\lambda}_3 = 0.43426$  and  $\bar{\lambda}_4 = 0.32569$ .

For the three node network, two stable wave-like oscillatory patterns (clockwise and counter-clockwise waves) are found and the oscillation parameters are successfully determined. The accuracy of the MHB method and the derived oscillatory profiles for the coupling strength  $\gamma_3 = 1.01$  are presented in Table 1.

Table 1. Oscillatory profiles of the network represented by matrix  $\Gamma_3$ . Multi-stability.

Wave	Residual	$\Delta\alpha$ in %	$\Delta\omega$ in %	$\omega$	$\alpha_e$	$\phi_1$	$\phi_2$	$\phi_3$
Clockwise	9.9256e-07	0.5781	0.0371	0.8365	0.1296	0	240	120
Counterclockwise	9.9256e-07	0.5781	0.0371	0.8365	0.1296	0	120	240

For the four node network, one wave-like solution is predicted. The predicted solution corresponds to a partial synchronization regime. We can observe synchronous behavior between two pairs of nodes, namely between the 1st and the 3rd, and between the 2nd and the 4th. Moreover, these pairs are in anti-phase synchronization with respect to each other. The accuracy of the MHB method and the predicted oscillatory profile for the coupling strength  $\gamma_4 = 1.01$  are provided in Table 2.

Table 2. Oscillatory profile and comparison of the MHB method and ODE simulation of the network represented by matrix  $\Gamma_4$ .

Residual	$\Delta\alpha$ in %	$\Delta\omega$ in %	$\omega$	$\alpha_e$	$\phi_1$	$\phi_2$	$\phi_3$	$\phi_4$
1.0171e-06	1.0793	0.0521	0.8362	0.1159	0	180	0	180

In the case of the four node network, the MHB method predicts the result which was previously obtained by means of the direct Lyapunov method in [Pogromsky *et al.*, 2011]. For the three node case, the analysis by means of the direct Lyapunov method is cumbersome due to the co-existence of two stable solutions.

Figure 8 shows that in the initial period of time the oscillations computed by the simulation and the output of the MHB method do not match because of transient effects. When the transients have sufficiently decayed the outputs are almost identical which implies that the MHB method accurately describes the patterns occurring in the networks. The vertical axis stands for the mismatch between outputs of the simulation and the MHB method and the mismatch is computed as  $e(t) = z(t) - q(t)$ . For some initial conditions, oscillations computed by the MHB method have different initial phases compared to the simulation ones. In order to compensate for this difference, an initial phase offset  $\phi_0$  can be applied to the MHB output vector as shown in (7).

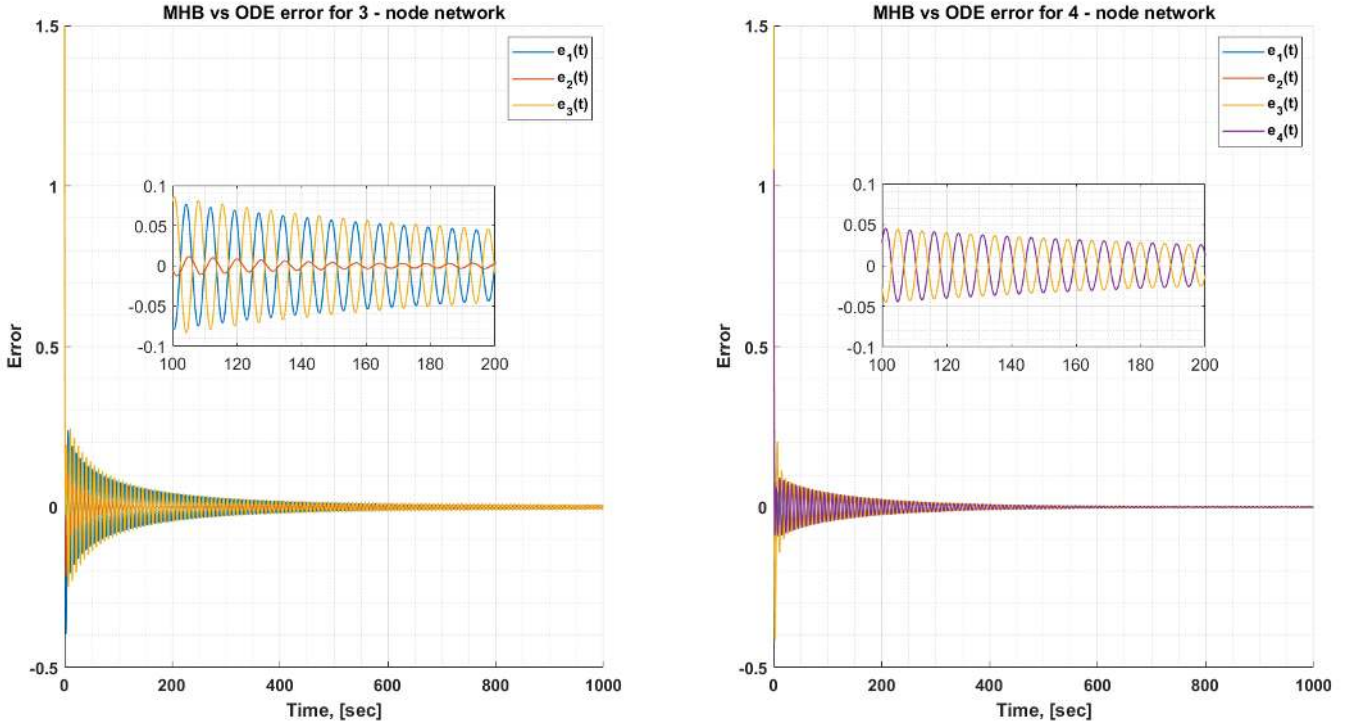


Fig. 8. Error between the MHB method and ODE simulations for three- and four-node networks for  $\gamma_{3,4} = 1.01\bar{\lambda}_{3,4}$ . Inner plots represent zoomed-in sections for the presentation purposes.

#### 4.2. Results for the general amplitude case

In this subsection, the results obtained by means of the optimization tools are presented. The numerical approach seeks for the set of the phases, amplitudes, and frequency that solves equation (14). This optimization method can also be applied to the equal amplitude case, at the cost of higher computation time. In the equal amplitude case the structure of the network can be exploited in such a way that one ends up with an eigenvalue problem of size  $n$  instead of  $nk$ .

Here we present the analysis of the networks which are given in Figure 6 and whose structure is described by matrices  $\Gamma_6$  and  $\Gamma_8$  where a subscript denotes the number of nodes in the network:

$$\Gamma_6 = \gamma_6 \begin{pmatrix} 3 & -1 & -1 & -1 & 0 & 0 \\ -1 & 3 & -1 & 0 & -1 & 0 \\ -1 & -1 & 3 & 0 & 0 & -1 \\ -1 & 0 & 0 & 1 & 0 & 0 \\ 0 & -1 & 0 & 0 & 1 & 0 \\ 0 & 0 & -1 & 0 & 0 & 1 \end{pmatrix}, \quad \Gamma_8 = \gamma_8 \begin{pmatrix} 3 & -1 & 0 & -1 & -1 & 0 & 0 & 0 \\ -1 & 3 & -1 & 0 & 0 & -1 & 0 & 0 \\ 0 & -1 & 3 & -1 & 0 & 0 & -1 & 0 \\ -1 & 0 & -1 & 3 & 0 & 0 & 0 & -1 \\ -1 & 0 & 0 & 0 & 1 & 0 & 0 & 0 \\ 0 & -1 & 0 & 0 & 0 & 1 & 0 & 0 \\ 0 & 0 & -1 & 0 & 0 & 0 & 1 & 0 \\ 0 & 0 & 0 & -1 & 0 & 0 & 0 & 1 \end{pmatrix},$$

where  $\gamma_{6,8}$  are bifurcation parameters. The Hopf bifurcation (equivariant Hopf bifurcation) occurs in these networks when the largest eigenvalue of matrix  $\Gamma_{6,8}$  exceeds  $\bar{\lambda}_6 = 0.30278$  and  $\bar{\lambda}_8 = 0.24881$  for the six node network and the eight node network, respectively.

We use the MultiStart optimization framework in order to predict patterns that appear in the given networks. The objective function is given in (21), without loss of generality, we set the first phase  $\phi_1 = 0$  in order to simplify the problem, and boundaries are chosen to be  $\phi_j \in [0, 2\pi] \forall j \neq 1$ ,  $\alpha_j \in [0, \beta] \forall j$ ,  $\omega \in [0, 2\omega_{bif}]$ , where  $\omega_{bif 6,8} = 0.8350$  derived from the bifurcation condition and  $\beta = 0.2$  is heuristically chosen. In order to show the accuracy of the MHB method for the general amplitude case, an error analysis is performed. First, we present the results for the network of six nodes and the coupling strength parameter  $\gamma_6 = 1.01$ . The procedure starts from ten random points within



the chosen domain and two distinct solutions are found that represent the clockwise and counter-clockwise waves. Existence of these waves implies the multi-stability of the network dynamics. The determined oscillatory patterns are given in Table 3 and the accuracy of the method is given in Table 4.

Table 3. Oscillatory profiles of the network represented by matrix  $\Gamma_6$ . Multi-stability.

Wave	$\omega$	$\alpha_1$	$\alpha_2$	$\alpha_3$	$\alpha_4$	$\alpha_5$	$\alpha_6$	$\phi_1$	$\phi_2$	$\phi_3$	$\phi_4$	$\phi_5$	$\phi_6$
CW	0.8364	0.1226	0.1242	0.1242	0.0375	0.0380	0.0380	0	240	120	180	60	300
CCW	0.8364	0.1226	0.1242	0.1242	0.0375	0.0380	0.0380	0	120	240	180	300	60

Table 4. Comparison of the MHB method and ODE simulation applied to the network represented by matrix  $\Gamma_6$ . Multi-stability.

Wave	Residual	$\Delta\alpha$ in %	$\Delta\omega$ in %
CW	0.00016	2.5387	0.0499
CCW	0.00016	2.5080	0.0230

One can see that the multivariable harmonic balance method accurately predicts the oscillatory patterns which appear in such networks, even for co-existing patterns.

The objective function (21) has the argument  $g \in \mathbb{R}^{2k+1}$ . It is not possible to visualize a function of this dimension in 3D and that is why we provide cross-sections of the objective function. We change two (out of the  $2k+1$ ) variables within some range and fix the remaining variables. Figures 9 and 10 show cross-sections in order to display that the computed solutions correspond to local minima. Figure 10 shows that there exist local minima for the clockwise and counter-clockwise wave-like solutions which implies multi-stability of the network.

We have the same setting (ten random points within the chosen boundaries) for the eight node network whose structure is represented by coupling matrix  $\Gamma_8$ . Multi-stability is not observed in this network. The coupling strength parameter is chosen to be  $\gamma_8 = 1.01$ . The determined oscillatory pattern is provided in Table 5 and the accuracy of the method is given in Table 6.

Table 5. Oscillatory profile of the network represented by matrix  $\Gamma_8$ .

$\omega$	$\alpha_1$	$\alpha_2$	$\alpha_3$	$\alpha_4$	$\alpha_5$	$\alpha_6$	$\alpha_7$	$\alpha_8$	$\phi_1$	$\phi_2$	$\phi_3$	$\phi_4$	$\phi_5$	$\phi_6$	$\phi_7$	$\phi_8$
0.8363	0.1209	0.1209	0.1209	0.1209	0.0289	0.0289	0.0289	0.0289	0	180	0	180	180	0	180	0

In a network of an even number of nodes in a "core" ring, we observe a partial synchronization mode and a simple phase shift of 180 degrees. As it was mentioned above, the MHB method approximates a nonlinearity by a linear gain. Theoretically, the accuracy of the approximation becomes better as the network moves closer to a bifurcation point. We show how the accuracy changes when we increase the coupling strength. The example of eight nodes is used to illustrate this dependence and the results are presented in Table 7 and Figure 11. We run the method for the eight node network but for different coupling strength parameter  $\gamma_8$ . We performed six runs increasing  $\gamma_8$  from 1.01 till 1.5.

The numbers in Table 7 and Figure 11 illustrate that the accuracy changes as it was predicted and the mismatch

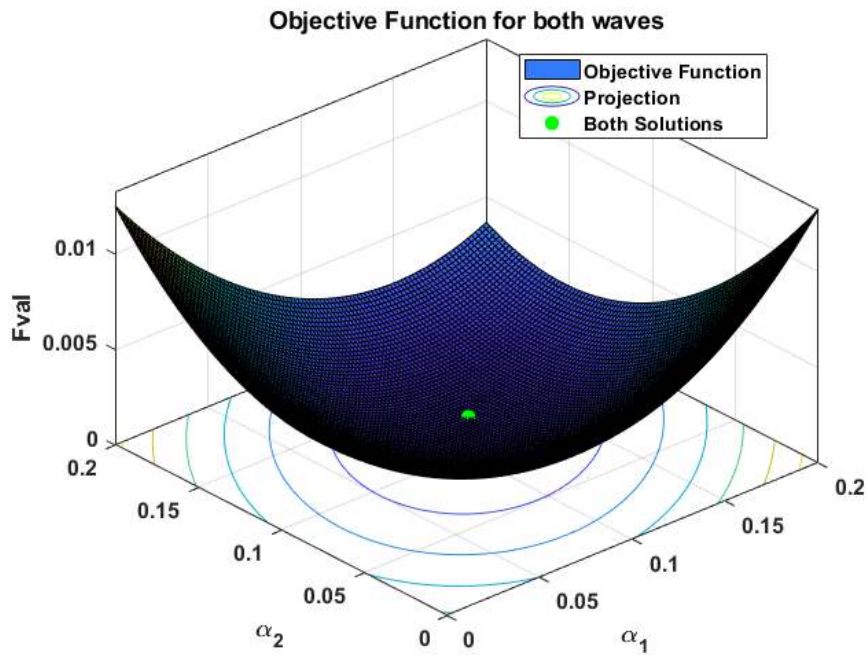


Fig. 9. Objective Function cross-section of  $\alpha_1$  and  $\alpha_2$  for clockwise and counterclockwise waves. Since both wave-like solutions has equal amplitudes  $\alpha_1$  and  $\alpha_2$ , they are shown as a single point.

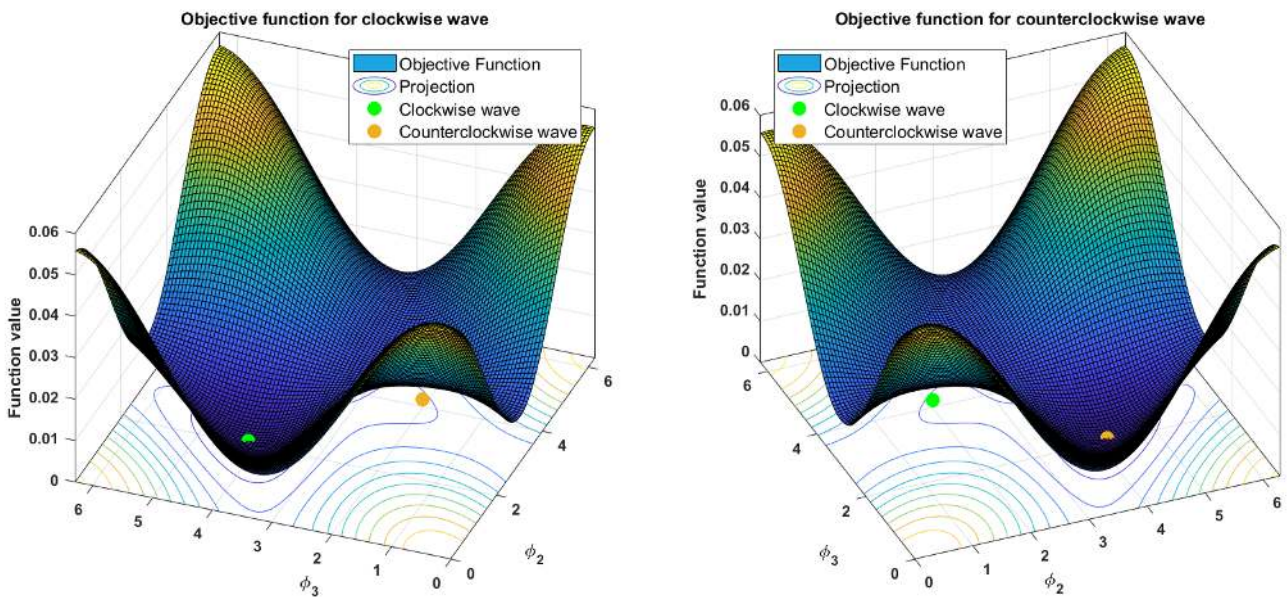


Fig. 10. Objective Function cross-section of  $\phi_2$  and  $\phi_3$  for both solutions.

increases when the system goes away from the Hopf bifurcation point. This data shows that the MHB method can accurately predict oscillatory patterns even if the system is "far" from the bifurcation point.

### 5. Conclusion

This work addresses the problem of predicting patterned oscillations of arbitrary amplitudes in networks of identical nonlinear dynamical systems of Lur'e form. The patterns are characterized by a set of parameters consisting of

Table 6. Comparison of the MHB method and ODE simulation applied to the network represented by matrix  $\Gamma_8$ .

Residual	$\Delta\alpha$ in %	$\Delta\omega$ in %
0.00056	2.4267	0.0367

Table 7. Comparison of the MHB method and ODE simulation for 8-n-node network vs. coupling strength.

Run	1	2	3	4	5	6
$\gamma$	1.01	1.1	1.2	1.3	1.4	1.5
Residual	0.0005	0.0003	0.0003	0.0003	0.0003	0.0568
$\Delta\omega$ in %	0.0127	0.0242	0.0798	0.1135	0.2266	0.3262
$\Delta\alpha$ in %	0.7264	0.7905	0.8440	0.9247	1.1635	1.2844

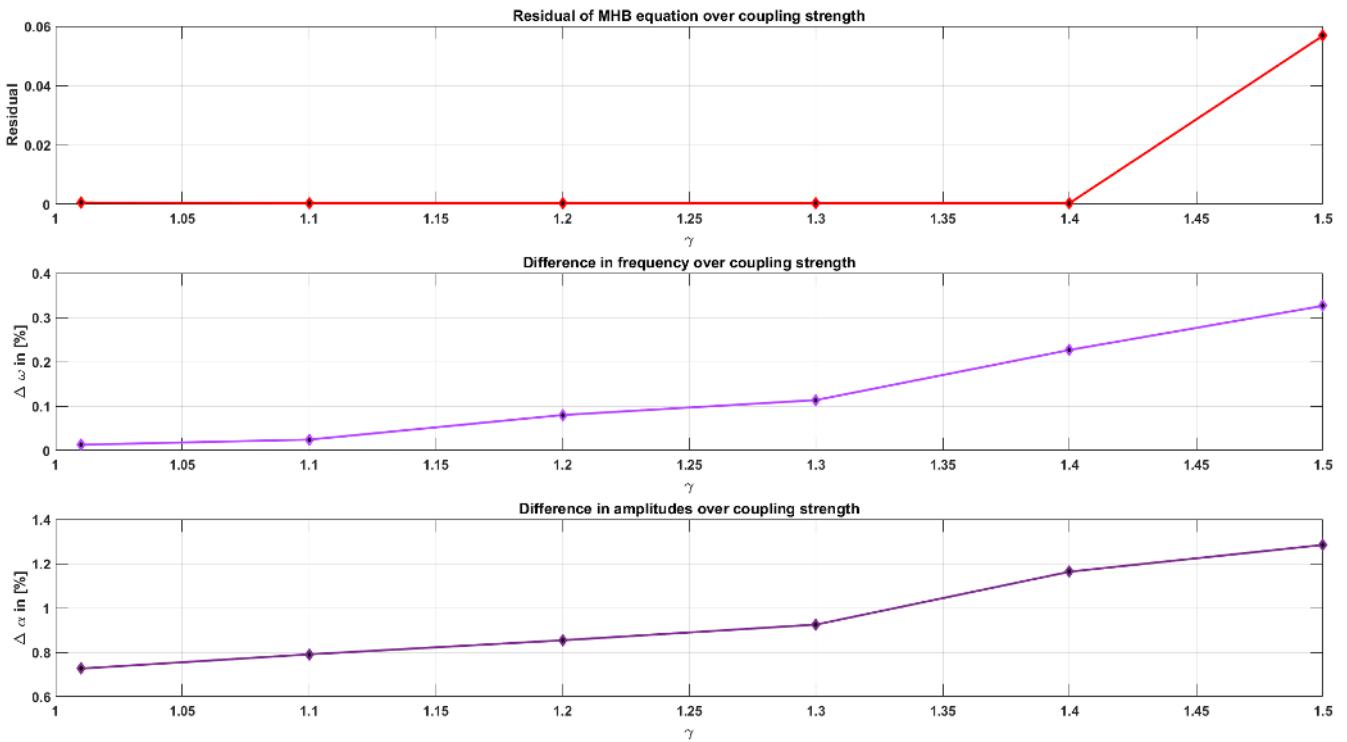


Fig. 11. Comparison of the MHB method and ODE simulation for network represented by  $\Gamma_8$  for different coupling strength.

frequency  $\omega$ , amplitudes  $\alpha_j$  and phases  $\phi_j$ . In this work, we consider the case when the Hopf bifurcation (equivariant Hopf bifurcation) is the origin of oscillations and the oscillations are sinusoidal-like in the neighbourhood of the bifurcation point. According to this the nonlinearity can be approximated by its describing function and the network behavior can be analyzed by means of the harmonic balance method. Moreover, these patterns may co-exist which implies multi-stability. Multi-stability makes the usage of common tools, such as the direct Lyapunov method, highly involved. The multivariable harmonic balance (MHB) method for coupled systems of specific class was presented in [Iwasaki, 2008]. The method is able to determine the oscillatory profile of patterns that occur in the network

of specific structure and deals with multi-stability. The MHB method is not directly applicable to the networks of interest and in this work, we present a modification of the MHB method for the networks consisting of the Lur'e systems coupled via diffusion. The multivariable harmonic balance equation for networks of Lur'e systems is derived and it is shown that the method can accurately predict patterns that are formed in the networks of diffusively coupled Lur'e systems. For this, two cases are considered the equal amplitude case and the general amplitude case. The equal amplitude case can be easily solved using structural properties of the network. The general amplitude case requires numerical analysis. A numerical optimization routine has been developed which determines optimal solutions to the MHB equation and therewith predicts all possible stable patterns of oscillations.

It is shown that the phenomenon of pattern formation occurring in networks of (diffusively) coupled Lur'e systems can be analysed by means of the multivariable harmonic balance method and the further research goal is to apply the MHB method to a collection of interconnected neuronal systems (e.g. FitzHugh–Nagumo model) with delays in coupling, which has been studied in [Steur & Pogromsky, 2017].

## Acknowledgements

The author received funding from the European Union's Horizon 2020 research and innovation programme under the Marie Skłodowska-Curie grant agreement No 675080.

## References

- Balanov, Z. [1997] "Equivariant Hopf Theorem," *Nonlinear Analysis: Theory, Methods and Applications* **30**, 3463–3474.
- Byrd, R. H., Gilbert, J. C. & Nocedal, J. [2000] "A trust region method based on interior point techniques for nonlinear programming," *Mathematical Programming* **89**, 149–185.
- Chen, W. [1997] *Graph Theory and Its Engineering Applications*, Advanced series in electrical and computer engineering (World Scientific).
- Dormand, J. R. & Prince, P. J. [1980] "A family of embedded Runge-Kutta formulae," *J. Comp. Appl. Math.* **6**, 1926.
- Dummit, D. S. & Foote, R. M. [1999] *Abstract Algebra (2nd ed.)* (New York: Wiley).
- Gershgorin, S. [1931] "Über die abgrenzung der eigenwerte einer matrix," *Bulletin de l'Académie des Sciences de l'URSS. Classe des sciences mathématiques et na* **6**, 749–754.
- Glad, T. & Ljung, L. [2000] *Control theory - multivariable and nonlinear methods* (Taylor and Francis).
- Golubitsky, M., Stewart, I., Buono, P.-I. & Collins, J. J. [1999] "Symmetry in locomotor central pattern generators and animal gaits," *Nature* **401**, 693–695.
- Gorban, A., Jarman, N., Steur, E., Nijmeijer, H., van Leeuwen, C. & Tyukin, I. [2015a] "Directed cycles and multi-stability of coherent dynamics in systems of coupled nonlinear oscillators," *IFAC-PapersOnLine* **48**, 19 – 24, 4th IFAC Conference on Analysis and Control of Chaotic Systems CHAOS 2015.
- Gorban, A., Jarman, N., Steur, E., van Leeuwen, C. & Tyukin, I. [2015b] "Leaders Do Not Look Back, or Do They?" *Math. Model. Nat. Phenom.* **10**, 212–231.
- Hale, J. [1997] "Diffusive coupling, dissipation, and synchronization," *Journal of Dynamics and Differential Equations* **9**, 1–52.
- Han, M. & Yu, P. [2012] "Hopf Bifurcation and Normal Form Computation," *Normal Forms, Melnikov Functions and Bifurcations of Limit Cycles* (Springer London), pp. 7–58.
- Iwasaki, T. [2008] "Multivariable harmonic balance for central pattern generators," *Automatica* **44**, 3061–3069.
- Khalil, H. K. [1996] *Nonlinear Systems* (Prentice-Hall, New Jersey).
- Kuznetsov, Y. A. [1998] *Elements of Applied Bifurcation Theory (2Nd Ed.)* (Springer-Verlag, Berlin, Heidelberg).
- Lowenstein, O. E., Osborne, M. & Wersll, J. [1964] "Structure and innervation of the sensory epithelia of the labyrinth in the thornback ray," *Proceedings of the Royal Society of London. Series B. Biological Sciences* **160**, 1–12.
- MATLAB [2017] *MATLAB Optimization Toolbox (R2017a)* (The MathWorks Inc., Natick, Massachusetts).
- Nakao, H. & Mikhailov, A. S. [2010] "Turing patterns in network-organized activator-inhibitor systems," *Nature Physics* **6**, 544–550.

- Pikovsky, A., Rosenblum, M. & Kurths, J. [2001] *Synchronization*, Cambridge Nonlinear Science Series (Cambridge University Press).
- Pogromsky, A., Glad, T. & Nijmeijer, H. [1999] “on Diffusion Driven Oscillations in Coupled Dynamical Systems,” *International Journal of Bifurcation and Chaos* **09**, 629–644.
- Pogromsky, A., Kuznetsov, N. & Leonov, G. [2011] “Pattern generation in diffusive networks: How do those brainless centipedes walk?” *Proceedings of the IEEE Conference on Decision and Control*, 7849–7854.
- Pogromsky, A. & Nijmeijer, H. [2001] “Cooperative oscillatory behavior of mutually coupled dynamical systems,” *IEEE Transactions on Circuits and Systems I: Fundamental Theory and Applications* **48**, 152–162.
- Rogov, K., Pogromsky, A., Steur, E., Michiels, W. & Nijmeijer, H. [2018] “Pattern prediction in networks of diffusively coupled nonlinear systems,” *IFAC-PapersOnLine* **51**, 62 – 67, 5th IFAC Conference on Analysis and Control of Chaotic Systems CHAOS 2018.
- Smale, S. [1976] “A Mathematical Model of Two Cells Via Turing’s Equation,” *The Hopf Bifurcation and Its Applications* (Springer New York), pp. 354–367.
- Steur, E. & Pogromsky, A. [2017] *Emergence of Oscillations in Networks of Time-Delay Coupled Inert Systems* (Springer International Publishing, Cham), pp. 137–154.
- Strogatz, S. [2003] *Sync: The Emerging Science of Spontaneous Order* (Hyperion Press).
- Tomberg, E. & Yakubovich, V. [2000] “On one problem of Smale,” *Siberian Mathematical Journal* **4**, 771–774.
- Turing, A. [1952] “The chemical basis of morphogenesis,” *Philosophical Transactions of the Royal Society of London. Series B, Biological Sciences* **237**, 37–72.
- Ugray, Z., Lasdon, L., Plummer, J., Glover, F., Kelly, J. & Mart, R. [2007] “Scatter search and local nlp solvers: A multistart framework for global optimization,” *INFORMS Journal on Computing* **19**, 328–340.
- Yakubovich, V. [1973] “Frequency conditions for auto-oscillations in nonlinear systems with one stationary nonlinearity,” *Siberian Mathematical Journal* **14**, 768–788.
- Yakubovich, V. & Tomberg, E. [1989] “Conditions for auto-oscillations in nonlinear systems,” *Siberian Mathematical Journal* **30**, 641–653.